Stars and their variability observed from space
C. Neiner, W. W. Weiss, D. Baade, R. E. Griffin, C. C. Lovekin, A. F. J. Moffat (eds)

Be STAR VARIABILITY AS SEEN FROM GROUND-BASED AND SPACE PHOTOMETRY

J. Labadie-Bartz[1] and A. C. Carciofi[1]

Abstract. Recent progress in understanding and modelling Be-star disk evolution is reviewed. Calculations of the angular momentum carried away by the disk provide a unique way to test certain predictions of stellar evolution models dealing with angular momentum transport. Knowing reasonably well how a disk behaves over months and years once formed, we can turn to recent and ongoing space photometry to classify Be star variability on shorter time-scales. Results from space missions have revealed that typically Be stars have much more complex frequency spectra than their non-Be siblings, showing features that, even though shared by other types of objects, are probably unique to Be stars in how they combine. From an initial analysis of 254 light-curves of southern Be stars observed by *TESS* with a 2-min cadence during its first year of operations, we identified 8 types of variability features, according to the properties of their light-curves and frequency spectra, and assigned each one visually to one or more of those types. By far the most common type of variability, present in 57–86% of the stars (depending on the spectral sub-type) is the presence of frequency groups. Other common features include isolated single frequencies and prominent stochastic variability. This work is a first step towards attempting to understand the complex frequency spectra of Be stars and their relation to what has so far been an elusive mass-loss mechanism operating in them.

Keywords: Techniques: photometric, stars: emission-line, Be, mass-loss, oscillations

1 Introduction

-Be stars are non-supergiant, non-radially pulsating, B-type stars that are rotatig near the critical limit. Their spectra exhibit emission lines which arise in a viscous, Keplerian, circumstellar "decretion" disk formed from ejected stellar mass in discrete events called "outbursts." These disks appear and disappear, and can be variable on time-scales from hours to decades. Be stars are valuable astrophysical laboratories for studying the effects of rapid rotation on stellar structure and evolution, pulsation-driven mass loss, the physics of viscous disks, and the transport of angular momentum from the stellar interior to the outer layers and to its removal from the system via the decretion disk (*e.g.*, Rivinius et al. 2013; Rímulo et al. 2018).

This contribution discussed recent advances in Be research stimulated by the availability of good-quality light-curves. On the one hand, ground-based observations provide the long time-baselines needed to track the entire process of disk formation and dissipation. The large number of light-curves available from surveys such as OGLE (Udalski et al. 1997) enable us to select a sizable sample of Be light-curves with simple, well-isolated disk events (see Sect. 2. On the other hand, space photometry delivers both the high degree of precision and the high cadence to reveal the minute changes in brightness associated with stellar pulsation. This is important because nonradial pulsation is often thought to play an integral role on how Be stars eject mass, possibly through interaction of multiple modes (Baade et al. 2016; Kurtz et al. 2015).

2 Current understanding of Be star disks

The disks of Be stars are their most defining characteristic. A significant amount of research has been dedicated to observing, modelling, and interpreting the growth, dynamics and dissipation of the line-emitting gas in the circumstellar environment (Rivinius et al. 2013). The Viscous Decretion Disk model (VDD; Lee et al. 1991; Carciofi 2011) has emerged as the best explanation for the various observed phenomena. In the VDD model, the process of building a disk begins with material being somehow ejected from the star. Viscous diffusion then acts to transport matter and angular momentum outwards, causing the disk to grow (at the expense of some material losing angular momentum and falling back onto the star). With a constant mass injection rate the

[1] Instituto de Astronomia, Geofísica e Ciências Atmosféricas, Universidade de São Paulo, São Paulo, Brazil

disk grows towards a steady state; is geometrically thin, rotates in a nearly Keplerian fashion, has roughly a power-law radial density profile, and has a complicated temperature structure. The main free parameters in the VDD model are viscosity (according to the alpha disk theory), and the injection rate of mass and angular momentum into the disk (which can be, and often is, highly variable with time).

Be star disks are the brightest and most accessible systems for studying disk physics, owing to the fact that Be stars are common (comprising ∼20% of all main-sequence B stars) and show variability on accessible time-scales. Lessons learned about viscosity from Be star disks are relevant for astrophysical disks at all scales, including protostellar disks, AGN and accretion disks. Modelling the time-dependent structure of Be star disks provides measurements of the viscosity parameter, which is an integral aspect of all astrophysical disks as it controls the time-scales over which the disk evolves.

In the context of stellar evolution, Be star disks have relevance in that they transport angular momentum out of the system. Stellar evolution theory predicts that as a massive star evolves, its convective core contracts and spins up, and if there is sufficient coupling between the core and envelope, angular momentum will be transported radially outwards. By the creation of a disk, angular momentum is removed from the outer layers of the star and carried out of the system entirely, whereby the star avoids super-critical rotation. In this scenario, the angular momentum transported from the core should match the angular momentum lost from the disk. The Geneva stellar-evolution models account for this (Granada et al. 2013) and predict angular momentum loss rates as a function of stellar mass averaged over the main-sequence life-time. Modelling Be star disks provides a way to test those predictions. Fig. 1 shows an example model light-curve for a Be star with varying mass and angular momentum loss rates, and the total amount of angular momentum lost by the star through the disk in those episodes.

VDD theory has been used to model disk events by involving a large grid of hydrodynamic models and a Monte Carlo Markov Chain (MCMC) radiative transfer code to compute a grid of synthetic light-curves. The latter were then fitted to photometric OGLE data (Udalski et al. 1997) through an MCMC technique, whereby the viscosity parameter and angular momentum flux through the build-up and dissipation of the disk were calculated (Rímulo et al. 2018). Figure 2 shows an example disk event that was modelled in that fashion. A key result of the work by Rímulo et al. (2018) was that the angular momentum loss rates measured in disk events may be up to ∼100 times smaller than predicted by the Geneva models. The predictions of those models are compared to the calculated angular momentum loss rates of Be stars in the SMC and LMC (and one in the Milky Way) in Fig. 3. The discrepancy is made worse by the fact that Be stars are observed to spend only a fraction of their main-sequence life-time building disks (i.e., their duty cycle is approximately 10–20% from a preliminary analysis of OGLE data of LMC stars; A. Figueiredo, priv. comm.). Since the efficiency of angular momentum transport in stellar-evolution models is a free parameter, it is possible that it has been overestimated in the case of rapidly rotating stars. Further modelling of the light-curves of Be stars may provide the means to calibrate the angular momentum transport efficiency empirically in such evolutionary models.

3 Interpreting observations of Be star systems

tBoth the central star and the disk are interesting astrophysical systems to study. The previous section relies on observations and models of the disk. While the star forms the disk, the evolution of the disk is largely independent of the star itself, being primarily influenced by the gravitational and radiation fields of the star. Once a disk is formed, the material forgets its history and evolves mainly through viscous forces. Meanwhile, the central star represents the best opportunity to study the physics of rapidly rotating main-sequence pulsating stars. In order to learn from the star or the disk, it is necessary to disentangle their relative contributions to a given observable. For example, in the disk modelling method outlined in the previous section, the photometric excess arising from circumstellar material is the relevant quantity. For such methods to succeed, the brightness of the star must first be subtracted. Likewise, studies involving the star itself must account properly for any observational contributions from the disk.

Certain observed variations can be attributed confidently to either the star or the disk. In terms of photometry, brightening or fading events that occur on time-scales of months or years are understood to be due to disk growth or dissipation (e.g. Fig. 2), while coherent, stable periodic signals on time-scales of around one day are best attributed to stellar pulsation. There are, however, many cases where the origins of photometric signals are ambiguous. The stellar rotation period, orbital period in the close circumstellar environment, and possible pulsational periods, are all very similar. Since many factors can influence the total brightness of the system (and other observables) in often complex and time-variable ways, care must be taken in interpreting photometric data.

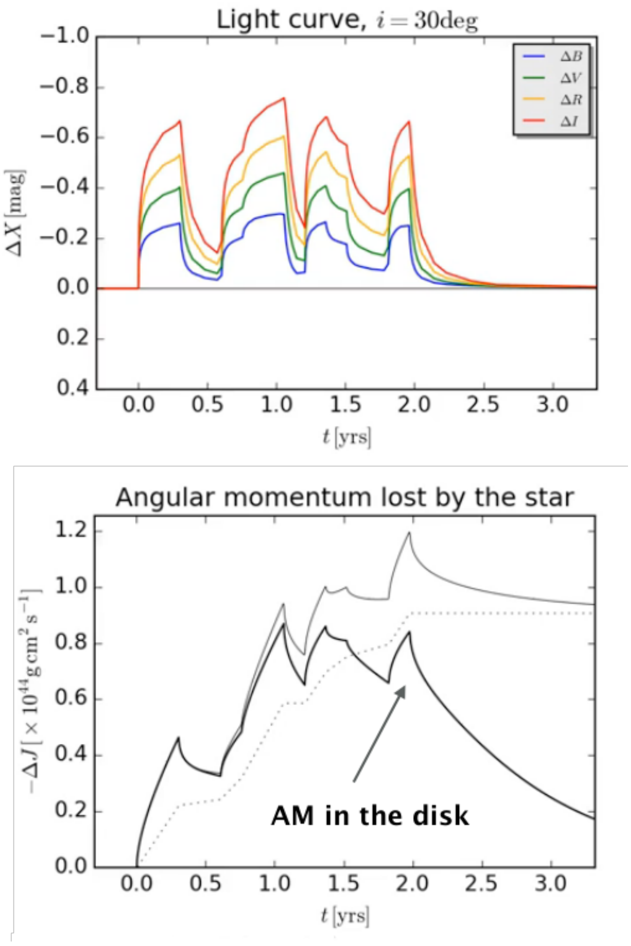

Fig. 1. Top: Simulated light-curve of a Be star with variable mass-loss rates, for several photometric bands, as indicated. When the brightness is increasing the Be star is ejecting mass and the disk is being built up. **Bottom:** The amount of angular momentum in the disk (solid black line) and the amount of angular momentum lost by a star (solid grey line) with the above simulated mass-loss history. As the disk dissipates it carries angular momentum out of the system.

Despite these complications, space photometry is a powerful tool that has opened a new window into understanding Be stars. In the following sections, we summarize recent progress and ongoing work from space photometry.

4 Space photometry of Be stars: recent highlights

Space photometry has led to significant advances in the field of classical Be stars in recent years. Analyses of space-based photometry have revealed that pulsation is ubiquitous among classical Be stars, and that they pulsate primarily in low order g-modes (Rivinius et al. 2003), similar to the class of Slowly Pulsating B (SPB) stars (Walker et al. 2005). Analyses of photometry from *MOST, BRITE, Kepler* and *CoRoT* have shown that the frequency spectra of Be stars are often complex relative to other B-type main-sequence pulsators (the β Cephei and SPB stars), typically exhibiting multiperiodicity, groups of closely spaced frequencies (as well as isolated frequencies), and signatures of stochastic variability (Baade et al. 2017, 2018; Rivinius et al. 2016; Semaan et al. 2018).

Frequency groups often appear in sets of three – one at low frequencies ($\sim$0.03 c d^{-1}), one at mid frequencies ($\sim$2 c d^{-1}), and the third at higher frequencies ($\sim$4 c d^{-1}). The high-frequency group is usually about twice the frequency of the mid-frequency group. Sometimes the mid-frequency group has two dominant frequencies whose difference roughly corresponds to the low-frequency group. While this general pattern is found in many Be stars, there are numerous exceptions. Nevertheless, in stars with these frequency groups, there can appear correlations between the frequencies and episodes of mass ejection (Baade et al. 2016), and are therefore prime

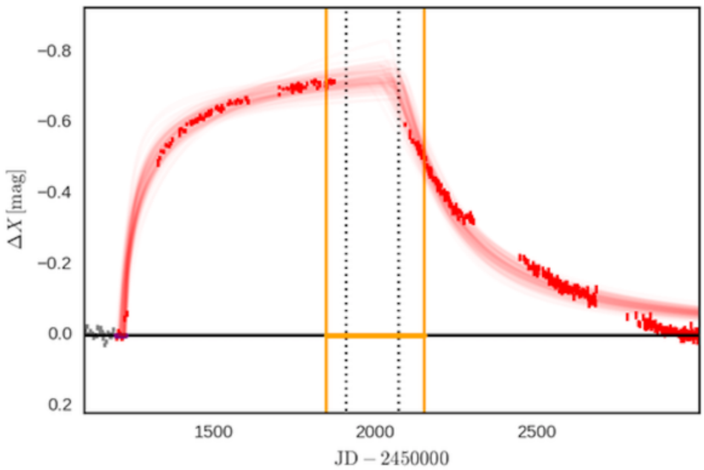

Fig. 2. Light-curve (red points; I band) of a disk event of an SMC star as seen with OGLE; the red lines represent 100 randomly chosen models from the MCMC routine. The vertical lines mark the range within which the MCMC sampler fits the transition of the disk phase from build-up to dissipation. Figure adapted from Rímulo et al. (2018).

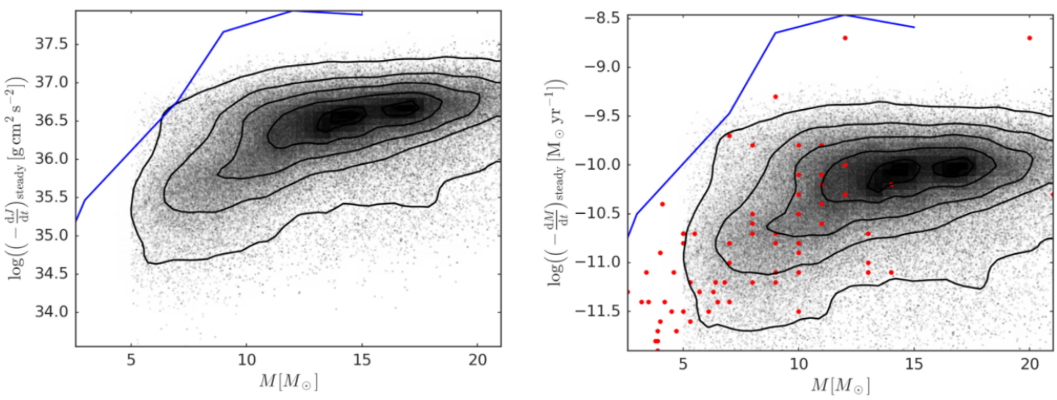

Fig. 3. Distributions of the steady-state mass (right) and angular momentum (left) loss rates for the sample of 54 Be stars from the SMC observed with OGLE. The blue curves show the predictions of the Geneva models for SMC metallicity from Granada et al. (2013) averaged over the main sequence life-time due to disk events. The red dots in the upper panel were computed for Galactic Be stars from Vieira et al. (2017). Figure reproduced from Rímulo et al. (2018).

objects for studying the mass ejection mechanism. One plausible hypothesis is that resonant mode coupling of pulsation modes can lead to combination frequencies with higher amplitudes than the sum of the base frequencies, which is somehow related to mass ejection (Rivinius et al. 2016).

It is well known that variability in both the stellar photosphere and the circumstellar environment can contribute to brightness changes and signals in the frequency spectrum. The frequency spectra often change drastically during active mass ejection episodes, with many transient modes appearing, variable amplitudes of the persistent modes, and characteristic signals at slightly lower frequencies than the stellar rotation (Semaan et al. 2018). An inhomogeneous distribution of recently ejected circumstellar material orbiting the star can leave such imprints on the frequency spectrum, but it is also possible that multiple transient pulsation modes are associated with these mass ejection events. From photometry alone it is difficult or impossible to disentangle the contributions from the photosphere and the circumstellar gas.

Great care must be taken in interpreting the frequency spectra as seen from space, since they are almost always time-variable. For example, it has been observed that during outbursts (here understood as an active disk-feeding phase), the amplitude of some modes increase, whereas in some modes the amplitude, frequency and phase may change (e.g., as seen in α Eri by Goss et al. 2011). Whether these changes in the frequency spectra are a cause or a consequence of the outbursts remains unknown. The disk may therefore add a layer of complication to the frequency spectrum that can only be investigated if the dynamical state of the disk (e.g., stability *versus* build-up *versus* dissipation) is understood properly. However, that can only be achieved if long-term multi-technique data are available.

5 Be stars with *TESS*

TESS is a space-based photometric mission designed to discover Earth-sized transiting exoplanets orbiting relatively bright stars by surveying nearly the whole sky. Launched on 2018 April 18, the nominal 2-year mission is dedicated to observing the southern ecliptic hemisphere for 1 year, followed by 1 year observing the northern ecliptic hemisphere. Each hemisphere is observed in 13 sectors, each with a 27 day base-line (but in overlap regions between sectors stars can be observed for many consecutive months, up to a full year). For stars brighter than $V = 8$ the typical precision is approximately 50 parts per million for 1 hour of observing. The observing cadence is 2 minutes for pre-selected targets (which can be requested through Guest Investigator programmes), and 30 minutes for the Full Frame Images (FFIs).

TESS is a unique space photometry mission for a number of reasons, but of particular relevance for massive stars is its nearly all-sky coverage and its focus is on bright stars ($5 < \mathrm{V} < 10$). While other space photometry missions such as *Kepler* and *CoRoT* observed some massive stars, the number is very small and the targets are faint, making detailed spectroscopic studies difficult or impossible. During its first two years *TESS* will observe approximately 1300 bright Be stars – a significantly greater number than all previous and current space missions combined. *TESS* therefore represents the best opportunity in the foreseeable future to study massive stars that vary on time-scales of days to weeks with photometry from space, since no similar missions are planned.

Our main goal in this section is to give a brief overview of the variability captured in the *TESS* light-curves of Be stars observed in the first year of the *TESS* mission. First, we identify and describe several characteristic features that appear in *TESS* data for our sample. Then we examine the light-curve and frequency spectrum for each object and record the types of signals shown. That provides us with information regarding the fraction of our sample showing various signals, and enables us to compare the features of the frequency spectra of the sample as a whole.

5.1 *Characteristic features of Be stars in TESS*

We begin by analyzing the light-curves of 254 classical Be stars observed with 2-minute cadence in the southern ecliptic in the first year of the *TESS* mission (Guest Investigator project ID G011204). For each light-curve, the Lomb-Scargle (LS) periodogram is also calculated as a measure of the frequency spectrum. While each light-curve and frequency spectrum is unique, there are certain features that are common among many members of the sample. Figure 4 shows examples of Be stars that exhibit these characteristic features, which are listed and described below.

- Type 1 – flickers: loosely defined as features in the light-curve whereby the brightness increases by a few percent over a few days, followed by a return towards the base-line. Some flickers show a precursor phase, i.e., a dimming before the rise in brightness, and some are accompanied by a temporary increase of the amplitude of higher-frequency signals (or their emergence if not already present). The largest amplitude features in panel B of Fig. 4, especially in the first half of the data, are examples of this. Flickers are not an oscillation around the mean brightness (like in panel A), but are rather a marked departure from the base-line brightness.

- Type 2 – Low-frequency signals dominate: the most prominent have frequencies lower than 0.5 c d^{-1} . Panels A and B in Fig. 4 show examples of stars with this characteristic.

- Type 3 – Stochastic variation: non-periodic, and a significant feature of the data. Stochastic signals can appear as extra noise in the frequency spectrum (as opposed to coherent periodic signals, which exist at a single frequency). However, this noise is astrophysical, and arises from genuine variability, which is not periodic. Wavelet analysis of these light-curves sometimes reveals real modes, albeit with varying amplitudes and frequencies. Panel C shows an example of this. The frequency spectrum between 0–2 c d^{-1} is characterized by stochastic variability in the data. There are also coherent and isolated signals at higher frequencies. Stochastic signals are likewise evident in the data in panel A, especially after removing the low-frequency signals ($<$ 0.5 c d^{-1}) from the data (grey lines in Fig. 4), and to a slightly lesser extent in panel B.

- Type 4 – Frequency groups: many closely-spaced frequencies that often form groups in the frequency spectra of Be stars. The light-curve in panel D shows three groups near 0.05, 1, and 2 c d^{-1} , panel E shows two groups near 3 and 6 c d^{-1} , and Panel B shows frequency groups where the first group at the lowest frequencies is highest in amplitude, and the other two groups centred around 1.5 and 2.5 c d^{-1} are relatively wide (and are more obvious after removing the low-frequency signals). The Be star in panel F also shows two prominent groups near 2.5 and 5 c d^{-1} .
- Type 5 – Single, isolated frequencies: single and well-defined in contrast to groups. There are many isolated frequencies in the periodogram of panel F, and also some in panel C.
- Type 6 – High-frequency signals: shown by some Be stars in contrast to theusual level, which is similar to that of the Slowly Pulsating B (SPB) stars, in that it is a g-mode pulsation with typical frequencies around 0.5–3 c d^{-1} . In this initial classification scheme, we have chosen 6 c d^{-1} as the defining level. Panel F shows a star with many high-frequency signals, while panels C and E are also examples that meet this criterion.
- Type 7 – Harmonics: a second frequency (or group) in the frequency spectrum occurs at twice the frequency of another signal. Some are exact, others are approximate. In panel D the group near 2 c d^{-1} could be considered the near harmonic of the group near 1 c d^{-1} , and likewise with the two groups in panel E. An exact harmonic is seen in panel F, where the lowest frequency, $f_0 = 1.684$ c d^{-1} has a first harmonic at $2\times f_0 = 3.368$ c d^{-1} .
- Type 8 – No variability: nothing above the *TESS* noise level in small fraction of the stars in the sample.

5.2 Analysis

We identified characteristic features of interest in the light-curves and frequency spectra, and inspected plots for the sample visually in order to determine which of the characteristics (above) could be attributed to each star. During this process we recorded the number of frequency groups and individual frequencies in each periodogram, and the frequency and amplitude of all significant signals* (having an S/N rate >4 using a 1.0 c d^{-1} window centred on the frequency in question). In all cases, versions of the periodogram were calculated both with and without frequencies lower than 0.5 c d^{-1} , since in many systems low frequencies dominate, and make the detection of higher-frequency signals more difficult if they are not first removed.

The sample was also subdivided according to a rough spectral-type designation from the literature. "Early-B" stars have a spectral type of B3 and earlier, "mid-B" stars have spectral types of B4–B6, and "late-B" stars are B7 and later. Of the 254 Be stars in this sample, 12 do not have a spectral type in the literature adequate for classifying them in that detail (e.g., an assigned type is "Be").

5.3 Results

As is clear from the examples in Fig. 4, a given Be star can display many of the characteristic features listed above: see Table 1. Figure 5 displays histograms showing the number of frequency groups in the sample. The dominant frequencies of each star in the sample are shown in Fig. 6, ordered by the frequency of the signal with the highest amplitude (after removing low frequencies); the three smaller panels show the same plot split along the spectral-type categories.

Table 1, Fig. 5 and Fig. 6 leads to the following conclusions. We found that early-type stars tend to show the most dramatic variability on time-scales accessible with *TESS*, and are the most likely to show flickers (11%) and high-amplitude low-frequency variations (33%), in accordance with previous results showing that early-type Be stars are much more active than late-type ones (*e.g.*, Labadie-Bartz et al. 2017). They usually have frequency groups (86%), 3 groups being the most typical configuration. However, frequency groups are also very common in mid-type stars (79%), and in late-type stars to a slightly lesser extent (57%). Isolated single frequencies are more common towards later spectral sub-types. High frequencies have a more or less uniform incidence across spectral types (∼23%), which is somewhat surprising since high frequency β Cephei-type pulsation is generally found only in early B stars. Only two stars were apparently without any signals above the noise level of *TESS*;

*Some discretion must be applied, because frequency groups can be wide and populated with many peaks of similar amplitudes. The signal-to-noise ratio (S/N) of any particular peak in such a group may be low according to the usual conventions, even when the group as a whole is clearly far above the noise level.

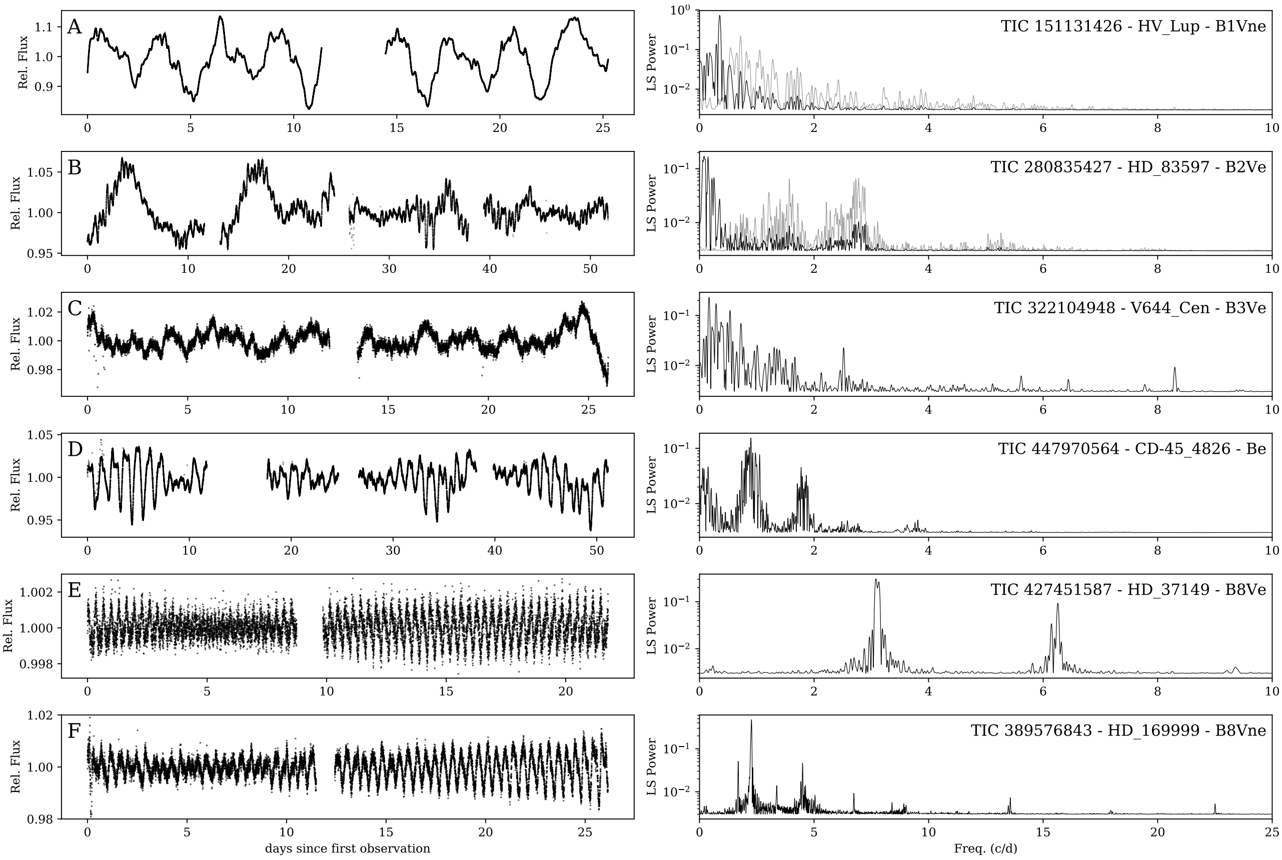

Fig. 4. *TESS* light-curves (**left**) and Lomb-Scargle periodograms (**right'**) for a representative selection of Be stars that show certain characteristic features, as described in the text. For the top two cases, the periodogram is re-calculated after removing the low frequency (< 0.5 c d^{-1}) signals and is shown in a lighter grey colour. Panels B and D show two sectors of *TESS* data; the rest have only one *TESS* sector of observations. The x-axis of the periodogram in panel F is extended to include the high frequencies. Signals at frequencies higher than 10 c d^{-1} are absent in all other stars shown here.

they require further analysis to derive upper limits to potential pulsational amplitude. Five stars appear to be mono-periodic, in that only a single frequency was found (with no harmonics) and they were without other types of variation. However, the short observational base-line of *TESS* and the possibility of signals below the detection threshold mean these are not necessarily purely single-mode pulsators.

Figure 6 shows a nearly linear crest between 0.5 and about 2.5 c d^{-1} . It means that within that frequency range the strongest frequencies seem to exist along a continuum, without any strong preference around any particular value. Groups associated with the strongest signal extend to both higher and lower values, but tend to have a longer tail towards lower frequencies. It is common for another group to exist at approximately twice the frequency of the dominant group. Exact harmonics of single frequencies are most common in the late-type stars, but it should be noted that late-type stars are less likely to have groups and more likely to have isolated frequencies dominant in their periodograms. Given frequency groups that do not have a single dominant frequency, it is difficult to distinguish the difference between exact harmonics and near harmonics. This introduces a bias in our analysis of harmonics in stars with frequency groups that has not yet been accounted for.

6 Conclusions

Ground-based photometric surveys have provided long-baseline light-curves of Be stars in the Galaxy, the SMC and the LMC. Some of the available light-curves are particularly well suited for disk studies, as they reveal the entire process of disk formation and dissipation. Recent such studies (Rímulo et al. 2018; Ghoreyshi et al. 2018) used these light-curves to determine the rate of angular momentum loss from the star in order to compare it

Table 1. Percentages showing variability classifications

	All (254)	*Early (126)*	*Mid (53)*	*Late (63)*
Flickers	7% (17)	11% (14)	6% (3)	0% (0)
Dominated by low freq. var.	22% (57)	33% (42)	19% (10)	6% (4)
Prominent stochastic variability	25% (63)	30% (38)	21% (11)	18% (11)
Frequency groups	77% (196)	86% (108)	79% (42)	57% (36)
Isolated single frequencies	40% (101)	33% (41)	43% (23)	50% (32)
High frequencies (> 6 c d^{-1})	23% (58)	22% (28)	23% (12)	24% (15)
Exact harmonics	15% (37)	9% (11)	17% (9)	25% (16)
No variability	1% (2)	0% (0)	1% (1)	1% (1)

Fraction of stars showing each type of variability, according to their spectral type. The category 'all' includes early-, mid-, and late-type stars, as well as 12 stars without a known spectral sub-type.

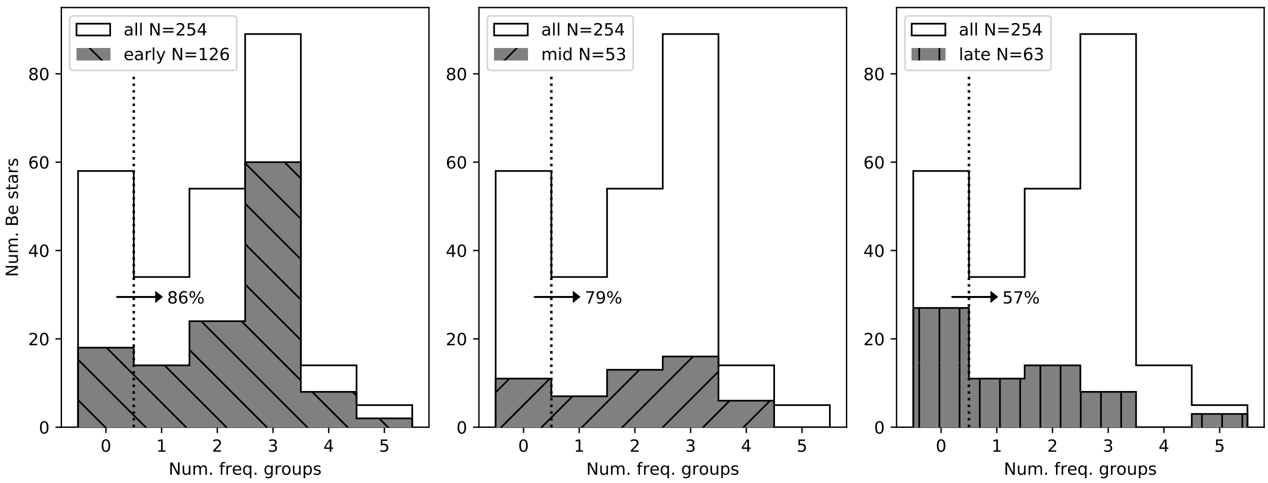

Fig. 5. Number of frequency groups in the Lomb-Scargle periodograms, split according to spectral sub-type. The black outline shows the distribution for the entire sample. In early-, mid-, and late-type stars, 86%, 79%, and 57%, respectively, show one or more frequency group.

with theoretical calculations from stellar evolution models of fast-spinning stars. The main result is that, even though the models do reproduce the observed trend of higher angular momentum loss rate for more massive stars, they predict rates that are up to 100 times larger than the observations reveal.

TESS promises to continue the legacy of massive-star photometry from space by providing by far the largest sample to date of high-precision, near-continuous data across nearly the entire sky. This is especially important for classical Be stars. Because Be star variability is so diverse and the phenomenon extends across a large range of spectral sub-types (late O to early A), large samples are needed to describe the behaviour of the Be-star population. This work takes a first step in that direction, by identifying characteristic signals that are seen in Be stars by *TESS*, and analyzing a subset of the southern Be stars observed in year 1 of *TESS* and ascribing their characteristics to each star (with most stars showing multiple features). Further work is being undertaken to define these characteristic signals more rigorously, to increase the sample size by including all southern Be stars (and not just 2-min cadence targets), to incorporate information from archived multi-year ground-based light-curves, spectroscopy, and the literature, and to acquire new spectra simultaneous with *TESS* observations to disentangle variability that arises in the photosphere rather than in the circumstellar environment.

J. L.-B. acknowledges support from FAPESP (grant 2017/23731-1). A. C. C acknowledges support from CNPq (grant 307594/2015-7) and FAPESP (grant 2018/04055-8).

References

Baade, D., Pigulski, A., Rivinius, T., et al. 2018, A&A, 610, A70

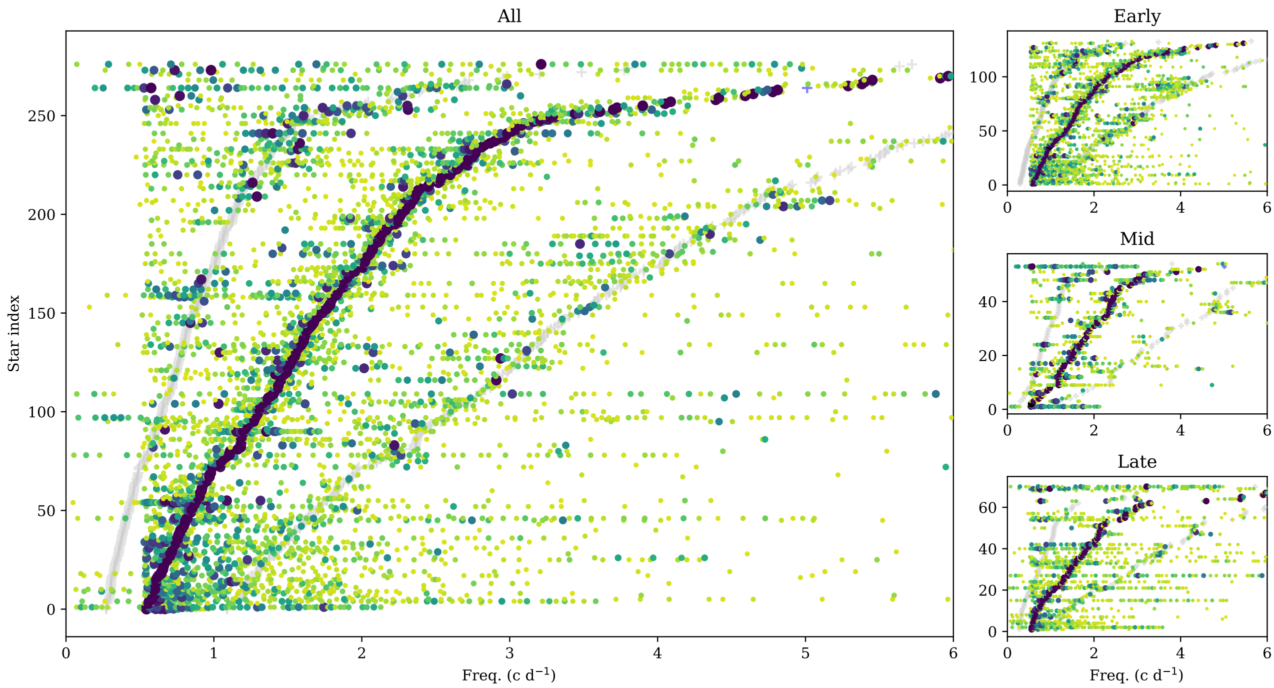

Fig. 6. Plots showing the strongest frequencies for the whole sample, sorted by spectral type. Each row in the plot shows the frequencies for one object. The stars are ordered according to their strongest frequency, increasing upwards. These frequencies are from a Lomb-Scargle periodogram, calculated after removing frequencies lower than 0.5 c d^{-1} . The grey lines to the left and right of the main frequency sequence are at 0.5 and 2*times* the strongest frequency, to help visualise signals that are near harmonics. Marker sizes and colour are proportional to the amplitude of the signal, relative to the strongest signal in each star (darker and larger symbols mean larger amplitude). There are many signals past the x-axis cutoff of 6 c d^{-1} but tend to be weaker, and the purpose of this plot is to show how frequencies lower than 6 c d^{-1} are distributed in the sample.

Baade, D., Rivinius, T., Pigulski, A., et al. 2017, in Second BRITE-Constellation Science Conference: Small Satellites - Big Science, Vol. 5, 196–205

Baade, D., Rivinius, T., Pigulski, A., et al. 2016, A&A, 588, A56

Carciofi, A. C. 2011, in IAU Symposium, Vol. 272, Active OB Stars: Structure, Evolution, Mass Loss, and Critical Limits, ed. C. Neiner, G. Wade, G. Meynet, & G. Peters, 325–336

Ghoreyshi, M. R., Carciofi, A. C., Rímulo, L. R., et al. 2018, MNRAS, 479, 2214

Goss, K. J. F., Karoff, C., Chaplin, W. J., Elsworth, Y., & Stevens, I. R. 2011, MNRAS, 411, 162

Granada, A., Ekström, S., Georgy, C., et al. 2013, A&A, 553, A25

Kurtz, D. W., Shibahashi, H., Murphy, S. J., Bedding, T. R., & Bowman, D. M. 2015, MNRAS, 450, 3015

Labadie-Bartz, J., Pepper, J., McSwain, M. V., et al. 2017, AJ, 153, 252

Lee, U., Osaki, Y., & Saio, H. 1991, MNRAS, 250, 432

Rímulo, L. R., Carciofi, A. C., Vieira, R. G., et al. 2018, MNRAS, 476, 3555

Rivinius, T., Baade, D., & Carciofi, A. C. 2016, A&A, 593, A106

Rivinius, T., Baade, D., & Štefl, S. 2003, A&A, 411, 229

Rivinius, T., Carciofi, A. C., & Martayan, C. 2013, A&A Rev., 21, 69

Semaan, T., Hubert, A. M., Zorec, J., et al. 2018, A&A, 613, A70

Udalski, A., Kubiak, M., & Szymanski, M. 1997, Acta Astron., 47, 319

Vieira, R. G., Carciofi, A. C., Bjorkman, J. E., et al. 2017, MNRAS, 464, 3071

Walker, G. A. H., Kuschnig, R., Matthews, J. M., et al. 2005, ApJ, 635, L77